Composites Part C: Open Access 5 (2021) 100157

Contents lists available at ScienceDirect

Composites Part C: Open Access

journal homepage: www.elsevier.com/locate/jcomc

Experimental study of adhesively bonded natural fibre composite – steel hybrid laminates

Karthik Ram Ramakrishnan*, Essi Sarlin, Mikko Kanerva, Mikko Hokka

Faculty of Engineering and Natural Sciences, Engineering Materials Science, Tampere University, POB 589, Tampere 33014, Finland

A B S T R A C T

Natural fibre composites (NFC), such as flax fibre reinforced plastics are green material with good specific properties. Significant research is currently in progress to improve the mechanical properties and durability of these composites and to make them competitive to traditional synthetic composites. A multi-material design approach is proposed in this study to develop a novel hybrid structure with a thin metal layer adhesively bonded to NFC. Two adhesives; a commercial epoxy adhesive and natural rubber were used for the adhesion between a stainless steel layer and flax composite with thermoset and thermoplastic matrix. The performance of the hybrid joint was investigated using a single lap joint (SLJ) test supported by full-field displacement measurement methods. The manufacturing of the composite specimen and the bonding of the NFC – metal joint with rubber adhesive was demonstrated. The force displacement curves from the SLJ test showed that the bonded joint with epoxy adhesive was stronger in comparison to the bonding with natural rubber. It is supported by the adherend failure observed in the joint with epoxy adhesive, while the rubber joint showed adhesive failure. The key outcome of the research is that the viability of adhesively bonded NFC - metal hybrid is established.

1. Introduction

The development of bio-based alternatives to traditional composite reinforcements is compelled by the critical need to address the challenges posed by global warming. Natural fibres from flax plant (Linum usitatissimum) are a renewable resource that entails less energy to manufacture and can help to fulfill our carbon emission reduction targets [1]. However, poor impact resistance and reduced long-term stability in outdoor conditions of these natural fibre composites (NFCs) pose a significant scientific challenge for researchers around the world. Hybridisation of NFCs, either with synthetic fibres or with metals is one of the potential keys to advance the mechanical performance of NFCs. Hybrid materials are lightweight structures that obtain improved functionalities such as vibration damping, and impact damage resistance by the combination of two or more materials [2]. Many researchers have studied hybrid materials and multi-material designs with composites and metal layers for applications in marine [3,4], automotive [5,6] and other industrial purposes [7]. In developing the assembly of dissimilar materials, the joining of the layers is very critical and the manufacturing of a durable interface within the hybrid structures is challenging due to the different physiochemical properties of the components [2]. Traditional joining technologies such as mechanical fasteners are not compatible with composite materials as fastener holes break the fibre continuity and introduce local stress concentration zones. Adhesive bonding is the most attractive joining method for the hybrid structures due to their high strength to weight ratio, more uniform stress distributions, waterproofing, and inhibition of galvanic corrosion [8]. However, adhesively bonded joints also have some disadvantages in that the bonding strength is quite sensitive to the surface preparation of the adherends and to environmental factors such as temperature and humidity [9]. In addition, they are difficult to disassemble for inspection, and therefore systematic studies on the failure and strength of these composite - metal bonded joints are a prerequisite for safe and reliable structural design. Webhe et al. [10] noted that the challenge in designing composite – metal hybrid parts is that the failure of the hybrid materials is more complicated than the failure of the bonded joints of monolithic materials as the failure can occur either in the composite itself (in fibre - matrix interface or interply) or in the interface layer with the metal.

Kim et al. [11] reported that despite the well-established literature on metal-to-metal bonded joints and composite-to-composite bonded joints, the joining of dissimilar materials is far less represented. Some researchers have studied the strength of adhesive bonding for steel and fibre reinforced polymer (FRP) composites [2,12–14]. Although successful composite-metal hybrid solutions have been developed for glass and carbon fibre composites, there is limited research on NFC hybrids. Kuan et al. [15] studied Fibre Metal Laminates (FML) with aluminium and various natural fibres and found that it was possible to improve the tensile and impact properties by hybridisation. Similarly, a considerable increase in the ballistic limit was observed for a steel-flax hybrid structure and it was reported that the energy dissipated by the hybrid material was comparable to or even better than mild steel [16]. Nevertheless, Santulli et al. [17] remarked that many challenges still remain in obtaining damage tolerance in natural FMLs that were comparable to synthetic FMLs. The adhesion between the metal and FRP layers was identified as a critical constraint. Campilho et al. [18] predicted the fracture performance of adhesive and co-cured joints in NFCs, but the adhesive bonding of NFC to metal layer is not thoroughly studied.

* Corresponding author.
E-mail address: karthik.ramakrishnan@bristol.ac.uk (K.R. Ramakrishnan).

https://doi.org/10.1016/j.jcomc.2021.100157
Received 18 January 2021; Received in revised form 9 April 2021; Accepted 17 May 2021

Budhe et al. [19] provided an extensive review of the recent literature on adhesively bonded joints in composite materials and identified the main factors that affected the failure mode and performance of adhesive joints as surface treatments, joint configuration, and geometric and material parameters. Anyfantis and Tsouvalis [12] reported that the standard test methods such as uniaxial tensile tests of Single Lap Joint (SLJ), Double Lap Joint, and Double Strap Joint were typically designed for adhesive joints of similar adherends but such standard procedures can also be applied for testing composite-to-metal adhesive joints. SLJ has emerged as the most common method for testing adhesive joints due to its simplicity [20]. Da Silva et al. [20] used the SLJ configuration to study different adhesive materials, thicknesses of the adherend and adhesive layers, overlap areas, surface treatments and durability. They found the overlap length to be the most critical factor on the lap shear strength. However, the eccentric loads in the single-lap joint configuration causes the adherends to bend, which generates high peel stresses in the adhesive, and therefore reduces the apparent shear strength of the adhesive joint. Sanz et al. [21] analysed the influence of geometric variations of the SLJ such as recessing and chamfering on the joint strength in terms of failure load, load eccentricity and the peak peel stress, and found that a gradual change of cross-section at the end of the overlap avoided the stress. Reis et al. [22] investigated the effect of the adherend stiffness and showed that the rigidity of the adherend had an inverse relation to the rotation of the specimen, which in turn promoted a more uniform stress distribution in the adhesive layer. It was also shown that in joints of dissimilar materials, the bond strength was determined by the adherend with lower stiffness [22]. Others studies have varied parameters like overlap length [8], surface roughness [3] and have shown the relationship between the failure loads, modes and bond lengths of the joints. Some studies such as those by Nunes [23], Sun et al. [24] and Moreira and Nunes [25] have applied full-field displacement measurement using high resolution CCD cameras combined with Digital Image Correlation (DIC) to measure the shear strains at the interface of lap joint. Sun et al. [24] measured the strain distribution in the adhesive bondline using DIC and showed that the shear and peel strains were the main constituents affecting joint failure. The strain evolution from the DIC analysis revealed that in joints with dissimilar adherends, crack initiation occurred on the interface end of the weaker adherend, while the fracture process was symmetric for joints with same adherends.

The viability of a novel hybrid structure manufactured by adhesive bonding of a thin stainless steel layer to a natural fibre composite is investigated in this paper. Two different flax fibre reinforced composites, with thermoset and thermoplastic resin, were chosen for the NFC layer. Optical microscopy was employed to characterize the surface of the adherends. The adhesion between stainless steel layer and NFC was investigated using a single lap shear test and Digital Image Correlation (DIC) was used to study the shear failure of the adhesive bond. It has been reported that adhesion between stainless steel and polymeric materials, especially thermoplastic composites is generally poor, and better understanding of the behaviour of adhesive interfaces in composite hybrids is needed. Two different adhesives were used for bonding; a commercial epoxy adhesive and a natural rubber. Sarlin et al. [2,26] have demonstrated that a composite - metal hybrid structure can be formed by vulcanizing a thin rubber layer between the steel and composite layers. The advantage of using rubber as the adhesive layer is that they can be modified with additives to be adaptive for both metallic and polymeric adherends and can add value to the structure, such as improved damping or energy absorption properties [2]. Scotchweld DP460 toughened epoxy adhesive which has good peel, shear, and impact properties was used as a reference adhesive to produce the composite - metal hybrid samples to compare with the natural rubber adhesive.

2. Materials and methods

The materials chosen for this study were flax fibre composites with two different matrices; namely flax/polylactic acid (PLA) and flax/epoxy. The flax/PLA composite was manufactured from commingled flax/PLA fibre (Lincore® flax-PLA technical fabric FWCT2 PLA 440) supplied by Groupe Depestele, France in the form of a woven 2 × 2-twill fabric with areal density of 400 g/m^2. The materials chosen for the thermoset composite was Biotex Flax, which is made of twistless natural flax fibres woven in a balanced 2 × 2-twill architecture and a two part epoxy resin: Araldite LY5052 epoxy resin and Araldur 5052 polyamine hardener (supplied by Swiss composite, Switzerland). The fabric developed by Composites Evolution, UK has areal density of 400 g/m^2 and typical ply thickness of 0.45-0.8 mm. The thermoset matrix was made of resin and hardener mixed in the ratio of 100:38 by weight. A ferritic stainless steel supplied by Outokumpu Stainless Oyj, Finland was chosen for the 0.5 mm thick metal layer. A thin metal layer was chosen to reduce the overall weight of the hybrid laminate. 3M^{TM} Scotch-Weld^{TM} DP460, a two-part epoxy adhesive with an amine accelerator was used for the bonding of the steel and composite layers. The typical properties of the adhesive as provided by the supplier are an overlap shear strength of 31 MPa for joints cured at room temperature for 24 hours.

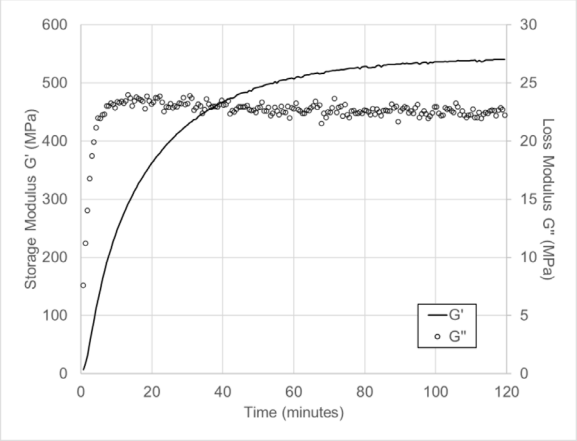

Fig. 1. Shear storage and loss modulus for natural rubber adhesive.

Natural rubber formulated by Teknikum Oy, Finland was used as the rubber adhesive. The cure conditions of the natural rubber were found using an Advanced Polymer Analyzer (APA2000) which is designed for testing viscoelastic materials for different temperatures, stresses, and frequencies. The vulcanization temperature chosen for this formulation was 150°C. A relatively low temperature was chosen to avoid the degradation of the flax fibres during the curing. The evolution of the shear storage and loss moduli of the natural rubber with increasing time at 150°C is shown in Figure 1. It can be seen that the shear loss modulus reaches equilibrium rapidly, but the storage modulus takes longer to achieve its asymptote. Based on the results, a curing time of 60 minutes at 150°C was chosen for the rubber adhesion.

There were four configurations of hybrid materials, namely:

1 Flax/PLA composite and stainless steel bonded with epoxy adhesive
2 Flax/epoxy composite and stainless steel bonded with epoxy adhesive
3 Flax/PLA composite and stainless steel bonded with rubber adhesive
4 Flax/epoxy composite and stainless steel bonded with rubber adhesive

2.1. Manufacturing of composite specimens

Square plates of 250 mm x 250 mm were manufactured using a hot press compression moulding system. The flax fabrics were dried at 60°C for 24 hours before fabrication in order to minimize the moisture content. Eight plies of the commingled flax/PLA fabric were placed in $[0/90]_8$ layup between the platens of a hot press for 5 minutes at a temperature of 200°C and a pressure of 40 bar as recommended by the

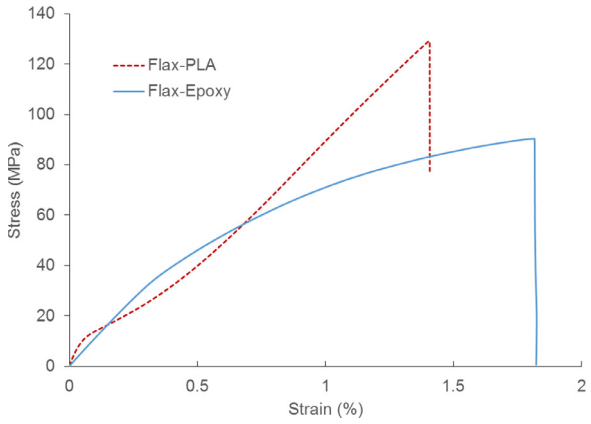

Fig. 2. Tensile stress-strain curve for the Natural Fibre Composites.

supplier. A peel ply was used to obtain rough surface to aid the bonding of the composite. The consolidated thermoplastic composite was cooled down to room temperature and was kept under pressure for another 12 hours. A wet layup process was used to manufacture the thermoset NFC, where 124.2 g of the epoxy resin/hardener mixture was used to impregnate four plies of Biotex flax fabric. The parameters for the press were 40 bar pressure without heating during 30 minutes. After that the composite was removed from the press and put under 10 kg weights (steel plate and weights) for 2 hours. The post-curing of the flax/epoxy composite was made in an oven at 50°C for 8 hours. The fibre volume fraction for both the flax/PLA and flax/epoxy composites was approximately 40%. The average thicknesses of the flax/PLA and flax/epoxy composites were 2.7 mm and 3.3 mm, respectively. The density of the flax/PLA and flax/epoxy composites were 1.22 ± 0.06 kg/m^3 and 1.07 ± 0.04 kg/m^3.

Uniaxial tensile tests of the natural fibre composites were performed following the guidelines of ISO 527-4 standard for mechanical characterisation of composite materials. The stress-strain curves for flax/PLA and flax/epoxy composites are shown in Figure 2. It can be seen that the tensile behaviour of the flax/PLA composite is quasi-linear with a brittle failure, while the flax/epoxy composite shows very nonlinear behaviour before brittle failure. The tensile modulus is computed from the slope of a linear trendline to the stress-strain curve in the range of strains between 0.05% and 0.3%. For flax/PLA composites, the average Young's modulus was 8.7 ± 0.7 GPa and the mean failure stress and strain were 123 ± 7 MPa and 1.3 ± 0.2 %, respectively. The flax/epoxy composite on the other hand, had an average Young's modulus of 9.5 ± 0.1 GPa and the failure stress and strain were 92 ± 6 MPa and 1.8 ± 0.4%, respectively.

2.2. Bonding of composite/steel layers

There are typically two kinds of bonding methods for composite to metal adhesive joints: co-curing and secondary bonding. Song et al. [9] studied the effects of the bonding methods on the joint strength and found that secondary bonded joints had comparable or higher strength than the co-bonded and co-cured joints. Therefore, a secondary bonding method was chosen. In this study, there are two types of bonded assembly: assembly with natural rubber and assembly with epoxy adhesive.

2.3. Surface preparation

Surface preparation is an essential pre-treatment for adhesive bonding to improve the bond strength between the substrates. For the steel adherend, the surface was first cleaned using acetone. It is necessary to increase the contact surface of the steel after cleaning by some mode of abrasion. The ideal method for this is grit blasting, but due to the thinness of the steel sheets (0.5 mm), the grit blasting caused the beam to warp and plastically deform. An alternative method of abrading with a sandpaper was used to create the rough contact surface. The steel was prepared with an abrasive paper 120 grit and cleaned with acetone. A comparison of the surface roughness of the steel sheet as received, treated with abrasive paper, and grit blasted is given in Figure 3. The micrographs show that both the abrasive paper and the grit blasting increase the roughness of the steel surface. The R_a values obtained from the Alicona InfiniteFocus G5 3D profilometer measurements of the surface roughness of the untreated, abrasive paper treated, and grit blasted surfaces were 0.12, 0.20, and 0.38 μm respectively.

The roughness of the surface has a bearing on the wettability of the material. The characterization of the wettability is typically performed by contact angle measurement establishing the tangent (angle) of a liquid drop on a solid surface, with high contact angle depicting hydrophobicity and low contact angles attraction of the liquid. The measurements were performed dynamically using a Drop Shape Analyser (Krüss DSA100). A motor-driven syringe was used to pump 5 µl droplet of UHP-grade water from MilliQ-system on the surface of the steel with different surface finishes, namely, smooth, abraded with abrasive paper and grit blasted surface. Figure 4 shows a typical droplet on untreated stainless steel surface and the measurement of the contact angle using an optical technique. The mean contact angle for untreated, abraded and grit blasted surface shows that the roughness increases the hydrophobicity compared to the untreated surface, which is evident from the increasing angle. The surface roughness and contact angle measurements show that an abraded surface of the stainless steel is suitable for adhesive bonding.

A similar analysis of the surface roughness of the composite samples was done using the Alicona profilometer. The optical microscope image and the depth measurements from the profilometer are shown in Figure 5. The fibre yarns and the woven structure of the composite is clearly visible. The R_a value for the composite was 3.35 μm indicating that the rough surface from the peel ply provides an ideal surface for bonding without additional surface treatment. A contact angle measurement of the composite was not successful as the surface was uneven and porous.

2.4. Experimental setup for the single lap joint test

2.4.1. Bonding of NFC – steel hybrids

The composite plate was cut to beams of dimensions 175 mm x 25 mm. A laser cutter was used for the thermoplastic composite while a Discotom 10 was used for the flax/epoxy composite. The 0.5 mm thick steel sheet was cut with a guillotine metal plate cutter. The geometry of the bonded sample for the single lap shear test is shown in Figure 6 (a). The single lap joint for composite - steel interface had an overlap length of 25 mm and a width of 25 mm. The adherend thickness was 0.5 mm for the steel and around 3 mm for the composite. For the assembly with epoxy adhesive, the two-part adhesive was applied using a 3M^{TM} Scotch-Weld^{TM} EPX^{TM} Plus II applicators with a duo-pack cartridge. A thin layer of the adhesive was spread on the adherend surfaces and the bonded sample was tightened with G-clamps for 24 hours at room temperature. The thickness was assured with metal shims. The epoxy bonded samples were allowed to fully cure for at least 24 hours before testing. For the hybrid samples bonded with rubber, a piece of rubber layer was placed between the composite and the steel layer and assembled as shown in the Figure 6 (b). Metal shims were placed between the samples to align the beams during curing and to maintain a uniform thickness of the bond. The assembly was placed in the press at 150°C with 40 bar for 1 hour. The measured adhesive layer thickness was 0.3 mm for epoxy adhesive and 0.6 mm for rubber. Additionally, alignment tabs were added to each sample (ASTM D1002) to guarantee the positioning of the joint during the test. The single lap joint (SLJ) shear tests were conducted with an Instron 5967 machine with a load cell of 2 kN and 30 kN. The crosshead displacement speed was 1 mm/min. At least three samples were tested for each configuration of adherends and adhesives.

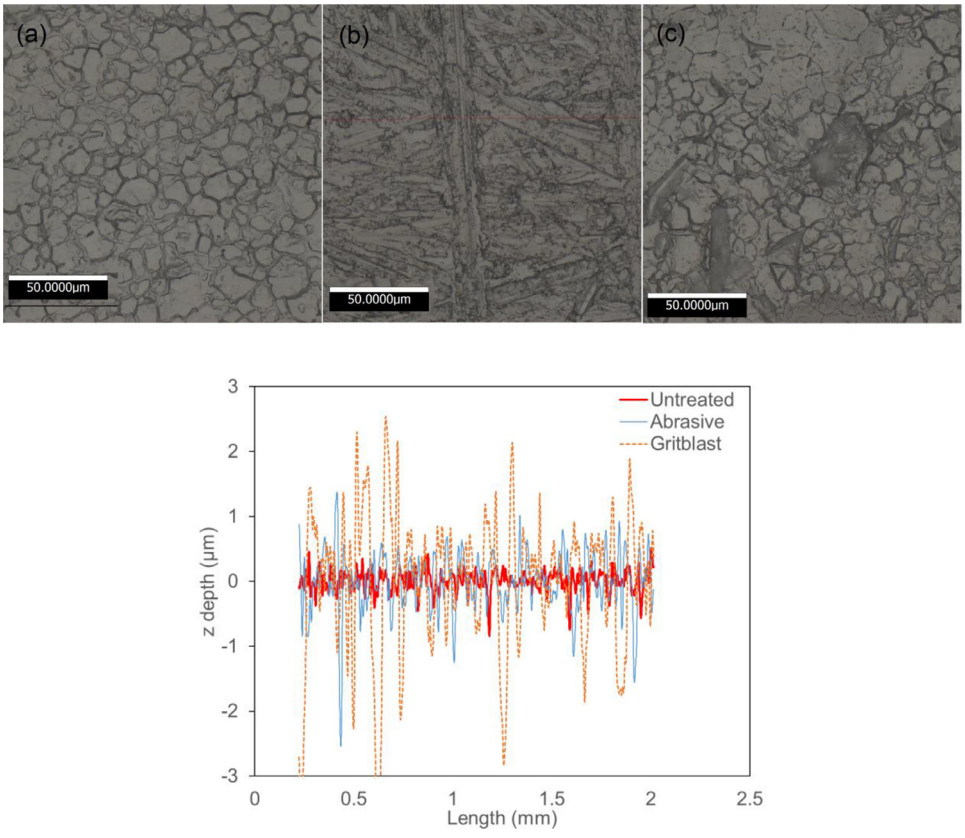

Fig. 3. Microscope image of the (a) untreated, (b) abraded and (c) grit blasted surface of the steel sheets and (d) comparison of the depth plot of the surfaces.

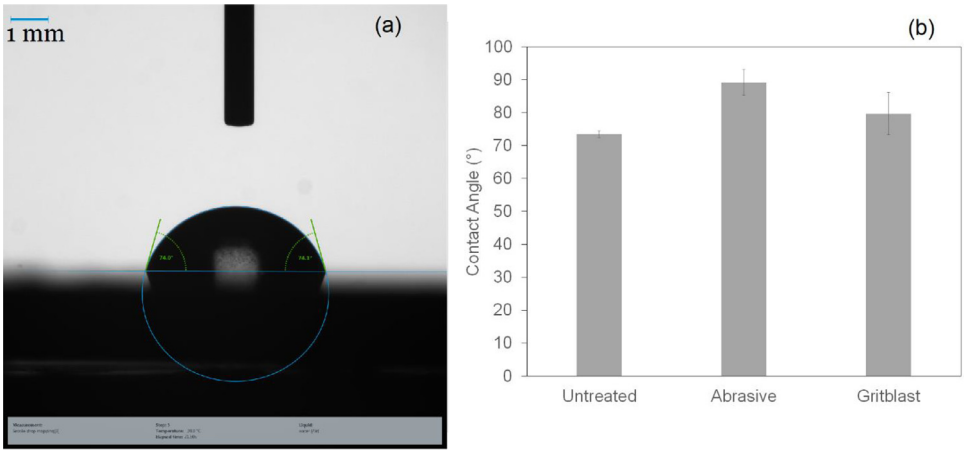

Fig. 4. (a) Typical droplet test for contact angle measurement and (b) Contact angle of the steel surfaces with different roughness.

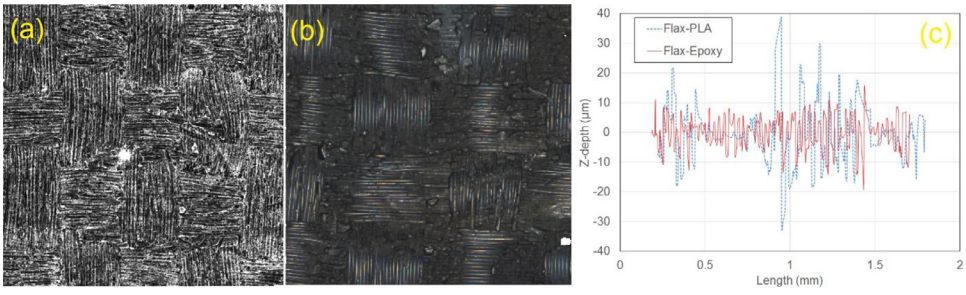

Fig. 5. Microscope image of (a) flax/PLA surface and (b) flax/epoxy surface, (c) comparison of depth plot.

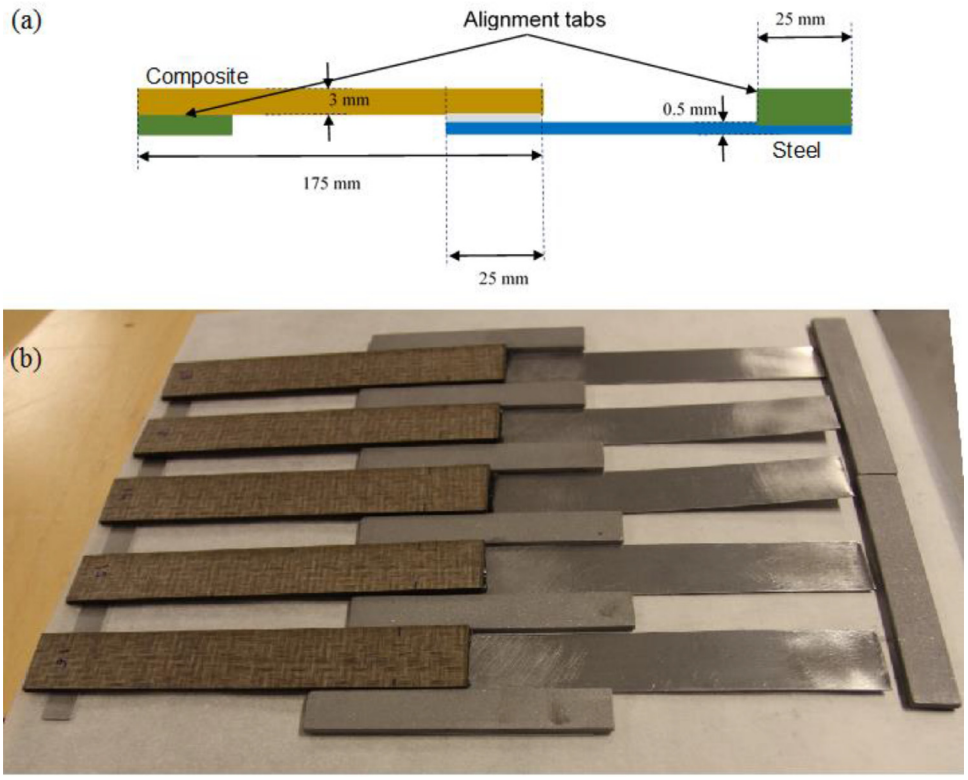

Fig. 6. (a) Single lap joint geometry and (b) bonding of the NFC and steel hybrid for single lap shear testing.

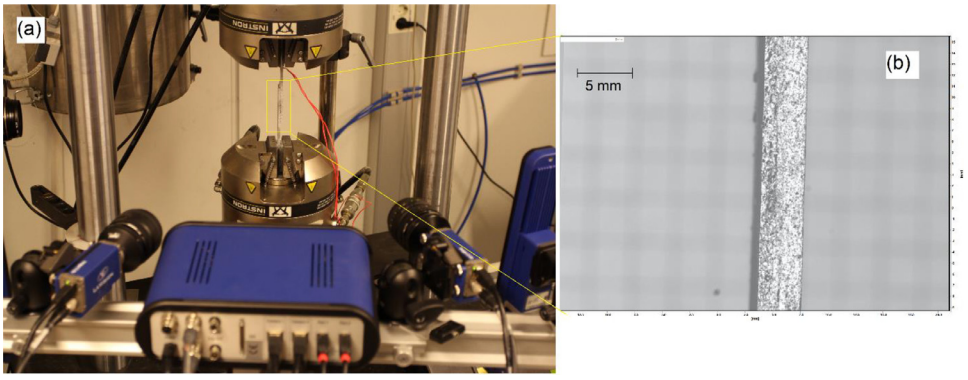

Fig. 7. (a) Single lap shear testing setup and (b) Speckled zone of interest.

2.4.2. Image acquisition

The Instron testing device was coupled with a LaVision digital image acquisition system with a Canon ultrasonic EF-100 mm lens. The experimental setup for the single lap shear test and specimen surface coated with a random pattern is shown in Figure 7. An airbrush was used to create a random speckled pattern on the surface of the bonded joint. A full-field 2D surface displacement measurement was implemented using Digital Image Correlation (DIC). The details of the camera setup and DIC parameters are provided in Table 1. A subset-matching DIC is an optical metrology technique based on comparing small areas of the digital images of reference or undeformed sample and successive deformed states to calculate full-field displacements and strains [23]. An Area of Interest (AOI) of 2456 × 400 pixels was chosen and the DIC analysis used a facet size of 25 × 25 pixels, and a step size of 9 pixels.

Table 1.
Specifications of the DIC system used in single lap shear testing.

Camera	Imager E-lite La Vision
Lens	Canon ultrasonic EF-100 mm lens
Lighting	LED array
Image size	2456 × 2058 pixels
Spatial resolution	1 mm = 57.23 pixels
Imaging distance	650 mm (approx.)
DIC Software	La Vision DaVis 8.3
Subset Size	25 pixels
Step Size	9 pixels
Sub-pixel interpolation	6th order spline
Virtual Strain Gage Size	59 Pixels = 1.03 mm
Subset Shape Function	2nd Order non-linear

3. Results and discussion

Figure 8 shows the load displacement curves for NFC-steel laminates bonded by epoxy adhesive. It can be seen that there is strong repeatability of the initial stiffness and the load at failure. For the epoxy adhesive, the flax/PLA hybrid shows a high peak load of 4100 ± 110 N, while the flax/epoxy hybrid shows a peak of 2925 ± 265 N. However, there is some scatter in the displacement at failure and the region after the inflection point can have different slope. The different changes in slope at the inflection point is hypothesized to be due to a bending moment

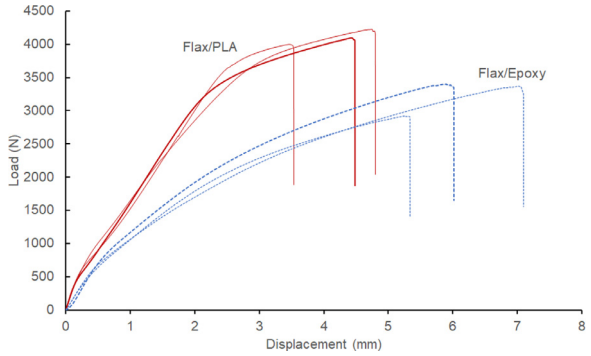

Fig. 8. Load-displacement curves (replicates) for flax/PLA and flax/epoxy NFC-steel bonded with epoxy adhesive.

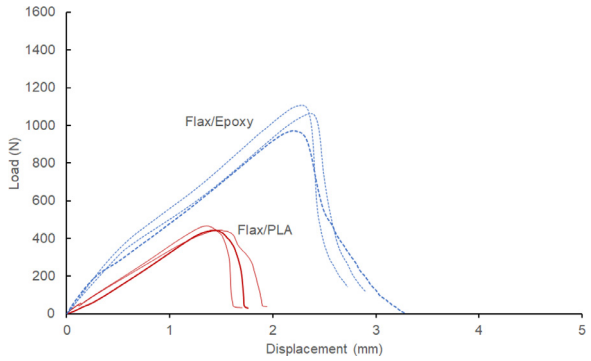

Fig. 9. Load-displacement curves (replicates) for flax/PLA and flax/epoxy NFC - steel joints with rubber adhesive.

caused by the asymmetry of thickness and stiffness of the adherends but it requires to be verified.

A similar comparison of the load displacement curves for flax/PLA and flax/epoxy composites bonded with rubber is shown in Figure 9. The peak loads of the rubber bonded joints for the flax/PLA and flax/epoxy composites were 445 ± 14 N and 1105 ± 132 N, respectively. It can be seen that the peak force for failure for the rubber adhesive joints is much lower compared to the epoxy adhesives. This clearly shows that the epoxy adhesive joint is much stronger than the rubber adhesive joint for the shear strength. The lower failure strength of the rubber adhesive for the flax/PLA composite also suggests that the use of natural rubber for adhesive bonding is more complicated for the thermoplastic and some chemical compatibilizer should be added. However, looking at the post-peak behaviour we can see that the epoxy adhesive has a brittle fracture, while the joint with rubber adhesive show a softening response like a slightly ductile adhesive.

The area under the load-displacement curve has been calculated and this energy to failure is taken as a performance parameter of the single-lap joints. The average energy to failure for flax/PLA and flax/epoxy NFC – steel joints with epoxy adhesive was 11.7 and 13.2 kN/mm, respectively. A similar energy calculation for rubber adhesive shows value of 0.45 and 1.6 kN/mm for flax/PLA and flax/epoxy NFC – steel joints. The average shear stress τ for a single lap joint is usually calculated as the applied load divided by the bond area, i.e. width of the bonded joint times the overlap length. The failure shear stress for epoxy adhesive was 6.3 and 4.2 MPa for flax/PLA and flax/epoxy composite. The rubber adhesive was much weaker and had a failure strength of 0.8 and 1.8 MPa for flax/PLA and flax/epoxy composite. It should also be noted that due to the adherend bending and induced peel loads, the peak shear stress found in the SLJ test is less than the true ultimate strength of the adhesive due to non-uniform stress distribution in the adhesive.

Optical observation of the lap joint at the end of the test was used to establish the mode of failure. It is well established that there are three different modes for the failure of the adhesive joint, namely, adhesive, cohesive, and mixed [4]. An adhesive failure appears at the boundary between the adhesive and adherends, while a cohesive failure occurs when the crack propagates within the adhesive layer. The mode is considered mixed when both failure modes occur simultaneously. The visual images of the failure surface of flax/PLA composite samples (Figure 10) confirms that the joint with the epoxy adhesives was stronger in shear strength, while the bonding with the rubber was poor. In the case of the epoxy adhesive (a,b), the failure occurs in the NFC adherend rather than at the interface. The rupture failure of the composite layer has occurred close to the overlap area and there is no damage in the steel substrate. However, for the rubber adhesive joints (figure 10 c and d), the failure occurs at the interface. It can be seen that the failure for the flax/PLA – rubber interface is an adhesive failure, as the surfaces of both adherends will have traces of the fractured adhesive in the case of a cohesive failure. This is an indication of the poor interaction between the natural rubber and the thermoplastic due to their chemical incompatibility and dissimilar chain structure. There is no evidence of residual pieces of rubber on the surface of the flax/PLA adherend after debonding. This confirms the need for some chemical compatibilization or other treatments such as plasma for improving the bonding between the thermoplastic and the rubber. It should be noted that there is no damage in the steel substrate. The excess adhesive that is squeezed out during the bonding forms a fillet in the composite in 10 (d), which sticks to the steel layer.

A similar analysis of the failure mode was done for the hybrid composite with flax/epoxy adherend. Figure 11 (a) shows that the epoxy bonded joint exhibited a combination of adhesive and cohesive failure as evidenced by the adhesive residue on both the substrates. This is an indication of good adhesion between the composite and the steel layer. This is further supported by adherend failure in the flax/epoxy composite for some cases as shown in Figure 11 (b), where the failure in the composite takes place away from the interface area. The rubber adhesive joint showed an adhesive failure similar to the flax/PLA case (Figure 11 c and d). This is consistent with the load displacement curves where the epoxy adhesive showed failure loads of almost 3 kN, while the rubber joint had a peak load of approximately 1 kN. However, it is important to observe that the adhesive failure of the rubber joint occurred at the interface between the steel adherend and rubber unlike in the flax/PLA composite where the failure occurred at the interface with the composite. This suggests that the natural rubber formulation is more suitable for thermoset composites than thermoplastics.

The different stages of a typical load displacement curve and the corresponding camera images showing the progression of joint failure is shown in Figure 12. The curve corresponds to a flax/epoxy – steel joint bonded with rubber. It can be seen from the load displacement curve that there are three regions; an initial linear region (1-2) followed by a change in the slope and finally a softening region. It can be seen from the camera images that the inflection point corresponds to the asymmetry in the thickness, which causes a small rotation. The load-displacement behaviour of the adhesive joint is therefore not a linear relationship but can be represented by a bilinear curve. At peak load, the adhesive joint has begun to fail and there is a drop in the force (point 3). The softening is an indication of the inability of the joint to carry further load and damage initiation and propagation in the adhesive layer. There is complete failure of the joint at point (4). The failure mechanism is mainly dominated by the debonding in the adherend-adhesive interface but other mechanisms such as plasticity of the rubber adhesive, microcracking, and void formation may also occur.

DIC analysis was conducted of the high resolution images to calculate the local displacement and strains. A typical progression of the displacement in the loading direction for a flax/epoxy composite bonded to the steel layer using natural rubber is shown in Figure 13. The displacement contours show that the displacement in the composite layer increases to

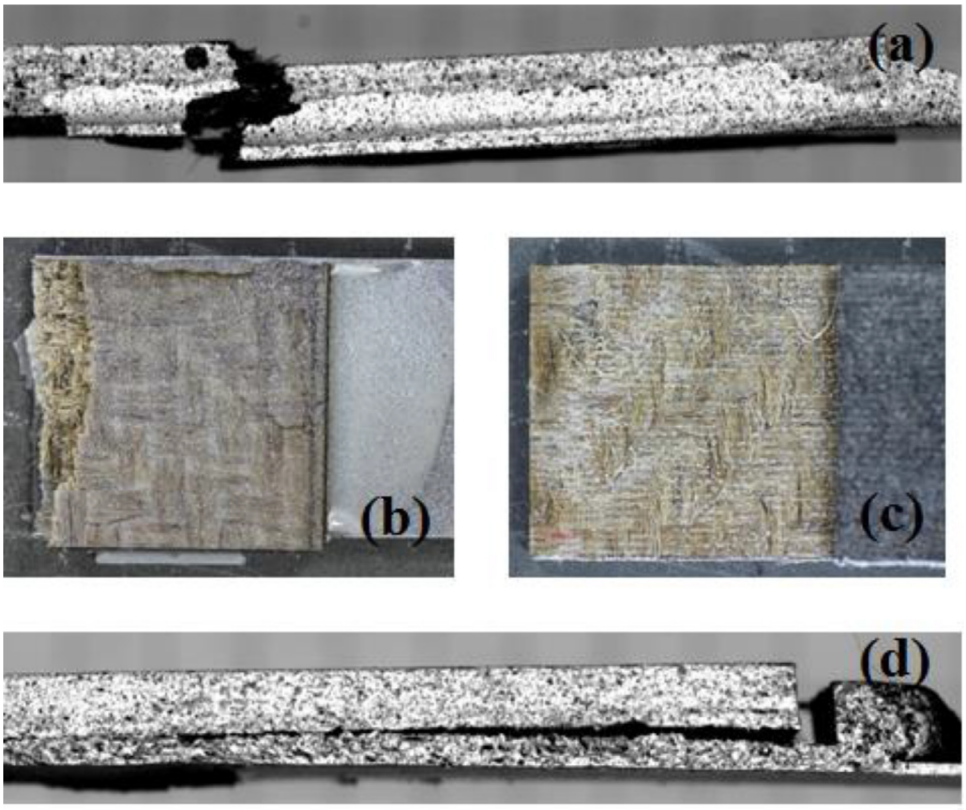

Fig. 10. Failure of the steel - flax/PLA joint with epoxy adhesive (a,b) and rubber (c,d).

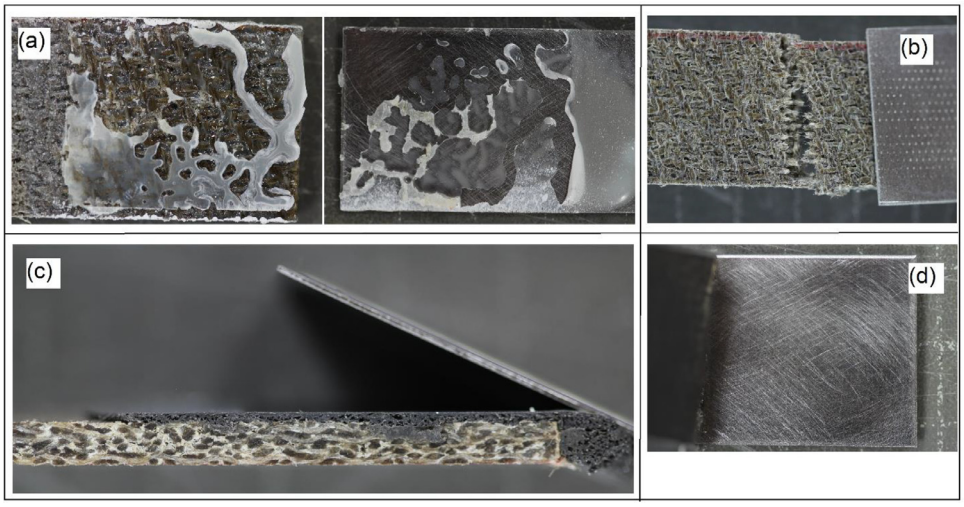

Fig. 11. Failure of the steel - flax/epoxy joint with epoxy adhesive (a,b) and rubber (c,d).

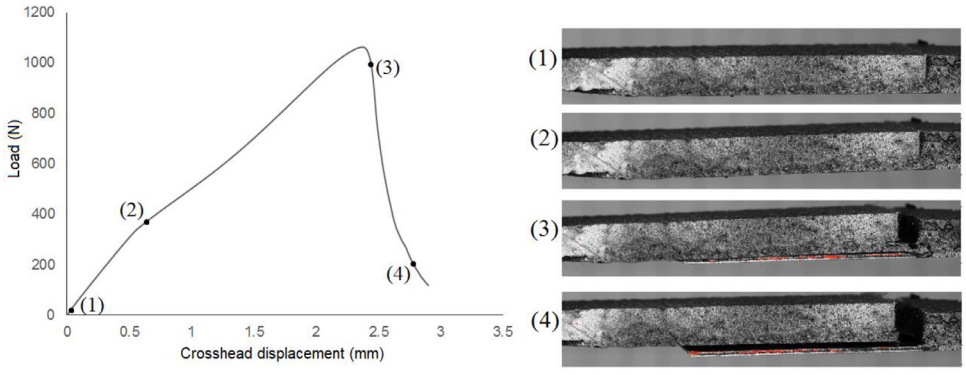

Fig. 12. Typical load-displacement curve and the progression of damage in the flax/epoxy-rubber - steel joint.

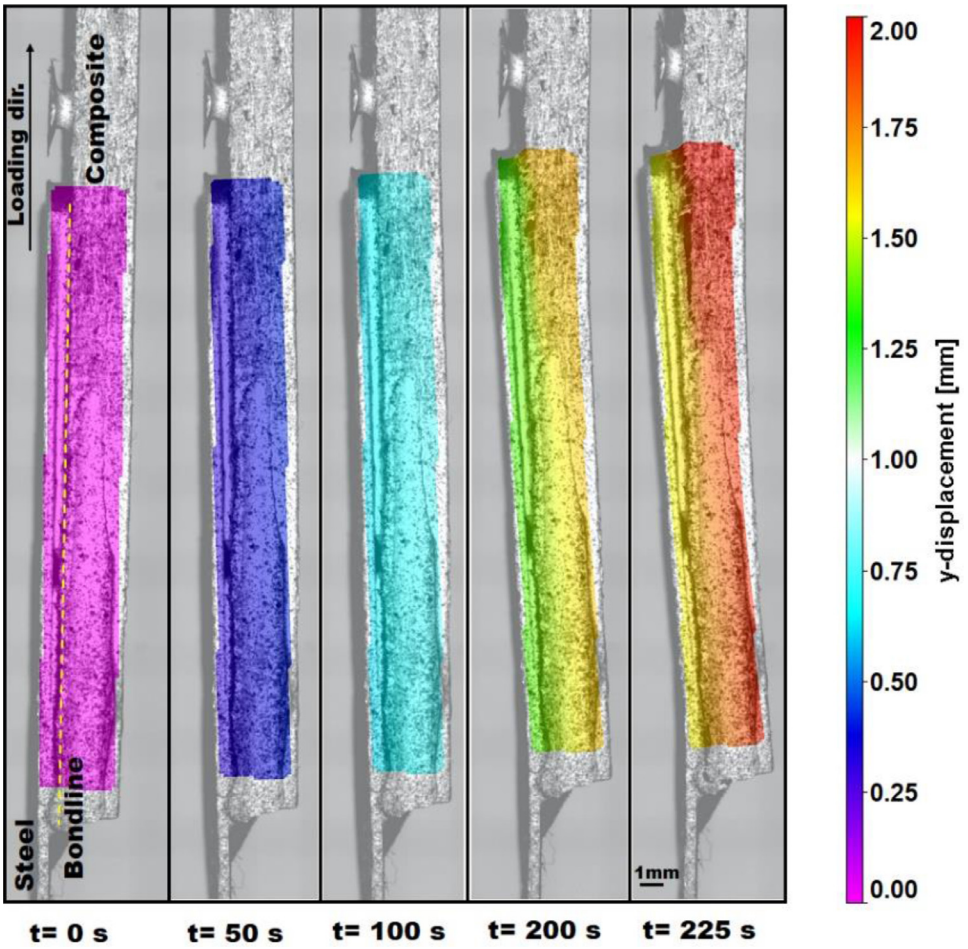

Fig. 13. Displacement contours for a single lap joint from DIC analysis.

approximately 2 mm before failure. The difference in the displacement of the two adherends is visible as differently colored contours on the steel and composite layer after 100 s. It can also be seen that despite using the alignment tabs, there is a small tilting of the sample for the bonded joint caused by the asymmetry of the thickness and stiffness of the two adherends. This displacement causes a combination of peel and shear stresses in the bonded area and the adhesive layer is not in pure shear.

Figure 14 shows the shear strain contour in the lap joint of the flax/epoxy (a,b) and flax PLA (c,d) for rubber and epoxy adhesive joints respectively. It can be seen that the thick and ductile rubber layer allows the visualization of the shear strains on the bonded joint, while the same is not true for the epoxy adhesive bonded joints. The failure in the case of the epoxy adhesive joint occurred in the composite adherend or mixed mode of failure.

The shear strain values obtained using a virtual strain gage along the length of the bondline of the flax/epoxy and flax/PLA composites bonded to steel layer using rubber and epoxy adhesive are shown in Figure 15. It can be seen that the strain response is highly nonlinear and that the failure strains for the epoxy adhesive are much higher than those observed for the rubber bonded samples. However, it can also be seen that while the adhesive bonded samples fail in a brittle manner with a sharp drop in the force, the rubber bonded samples show a gradual degradation of the strength even after initiation of the failure. This suggests that the rubber layer can be used as a ductile adhesive in applications where there is a lower shear strength requirement. It has been reported [27] that as long as the interfacial adhesion is on a reasonable level, the energy dissipation during impact is predominantly the plastic deformation of the metal layer and damage in the composite layer. Therefore the rationale to consider rubber adhesive for impact resistant structures is that a weak bond can still be used in impact applications and a ductile adhesive is able to redistribute the load over a larger area. The medium velocity impact resistance of flax composite hybrids with rubber interlayer will be presented in a subsequent article.

4. Conclusion

In this paper, the adhesive behaviour of natural fibre composite – steel hybrids was studied using single lap joint testing. Flax composites with PLA and epoxy matrix were fabricated and their uniaxial tensile properties were determined by tensile testing. A novel method to bond the thin stainless steel layer to the flax composite using a natural rubber as adhesive was investigated. A Scotchweld DP460 epoxy adhesive was used as a reference material for comparison. The surface preparation of the adherends was studied to maximize the bond strength. Single lap joint testing was conducted using an Instron testing machine and an image acquisition system. Digital Image Correlation (DIC) analysis was performed on the images to obtain strain contours of the bonded area. The force displacement curves from the lap joint test showed that the joint with flax/PLA composite and epoxy adhesive was stronger while the bonding with the rubber was poor. This was confirmed by observing the failed samples where the adherend failure for the epoxy adhesive joint and adhesive failure in the rubber samples could be observed. Similar behaviour was observed for the flax/epoxy composite, with the epoxy adhesive joint failing by adherend failure and the weaker rubber joint failing at the interface. The rubber layer while weak in shear, showed ductile characteristics and is potentially applicable in energy absorbing applications. Finite element modelling of the interface using

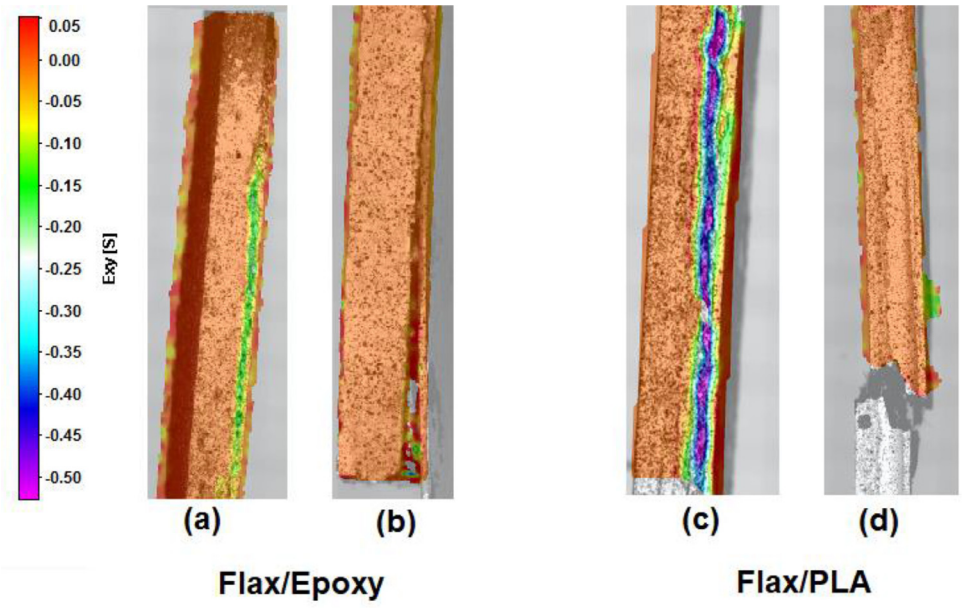

Fig. 14. Shear strain contours for the steel bonded to flax/epoxy with (a) rubber and (b) epoxy adhesive; flax-PLA composites with (c) rubber and (d) epoxy adhesive.

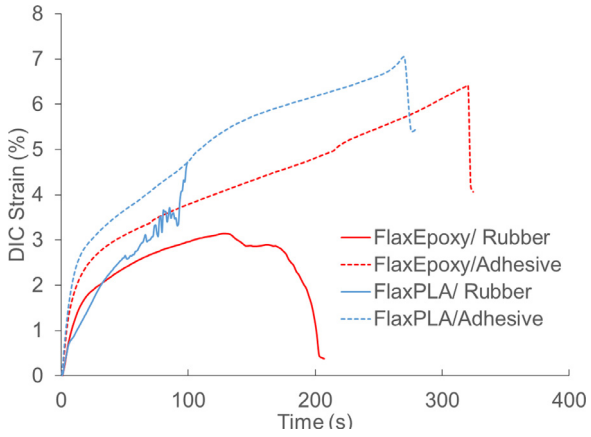

Fig. 15. Time history of shear strain obtained from DIC analysis.

cohesive elements is proposed for future work to focus on the failure in the interface.

Declaration of Competing Interest

The authors would like to thank Ms. Paivi Rita for her assistance in preparing the rubber used as adhesive in this project. Thanks are also due to Ms. Oriane Fillion and Mr. Olli Orell for their help in experimental setup.

Supplementary materials

Supplementary material associated with this article can be found, in the online version, at doi:10.1016/j.jcomc.2021.100157.

References

[1] A Bourmaud, J Beaugrand, DU Shah, V Placet, C. Baley, Towards the design of high-performance plant fibre composites, Prog. Mater Sci. 97 (2018) 347–408 https://doi.org/, doi:10.1016/j.pmatsci.2018.05.005.
[2] E Sarlin, E Heinonen, J Vuorinen, M Vippola, T. Lepistö, Adhesion properties of novel corrosion resistant hybrid structures, Int. J. Adhes. Adhes. 49 (2014) 51–57.
[3] Ç Özes, N. Neşer, Experimental Study on Steel to FRP Bonded Lap Joints in Marine Applications, Adv. Mater. Sci. Eng. (2015) 2015https://doi.org/, doi:10.1155/2015/164208.
[4] A Valenza, V Fiore, L. Fratini, Mechanical behaviour and failure modes of metal to composite adhesive joints for nautical applications, Int. J. Adv. Manuf. Technol. 53 (2011) 593–600 https://doi.org/, doi:10.1007/s00170-010-2866-1.
[5] JJM Machado, PMR Gamarra, EAS Marques, LFM. da Silva, Improvement in impact strength of composite joints for the automotive industry, Compos. Part B Eng. 138 (2018) 243–255 https://doi.org/, doi:10.1016/j.compositesb.2017.11.038.
[6] P Galvez, A Quesada, MA Martinez, J Abenojar, MJL Boada, V. Diaz, Study of the behaviour of adhesive joints of steel with CFRP for its application in bus structures, Compos. Part B Eng. 129 (2017) 41–46 https://doi.org/, doi:10.1016/j.compositesb.2017.07.018.
[7] JM Arenas, C Alía, JJ Narbón, R Ocaña, C. González, Considerations for the industrial application of structural adhesive joints in the aluminium-composite material bonding, Compos. Part B Eng. 44 (2013) 417–423 https://doi.org/, doi:10.1016/j.compositesb.2012.04.026.
[8] TEA Ribeiro, RDSG Campilho, LFM da Silva, L. Goglio, Damage analysis of composite-aluminium adhesively-bonded single-lap joints, Compos. Struct. 136 (2016) 25–33 https://doi.org/, doi:10.1016/j.compstruct.2015.09.054.
[9] MG Song, JH Kweon, JH Choi, JH Byun, MH Song, SJ Shin, et al., Effect of manufacturing methods on the shear strength of composite single-lap bonded joints, Compos. Struct. 92 (2010) 2194–2202 https://doi.org/, doi:10.1016/j.compstruct.2009.08.041.
[10] H Wehbe, D Blass, K. Dilger, Extracting a characteristic value concerning metal-composite-hybrids – identification of the relevant testing method, J. Adhes. 95 (2018) 1–19 https://doi.org/, doi:10.1080/00218464.2018.1562346.
[11] TH Kim, JH Kweon, JH. Choi, An experimental study on the effect of overlap length on the failure of composite-to-aluminum single-lap bonded joints, J. Reinf. Plast. Compos. 27 (2008) 1071–1081 https://doi.org/, doi:10.1177/0731684407087074.
[12] KN Anyfantis, NG. Tsouvalis, Loading and fracture response of CFRP-to-steel adhesively bonded joints with thick adherents - Part I: Experiments, Compos. Struct. 96 (2013) 850–857 https://doi.org/, doi:10.1016/j.compstruct.2012.08.060.
[13] M Giampaoli, V Terlizzi, M Rossi, G Chiappini, P. Munafò, Mechanical performances of GFRP-steel specimens bonded with different epoxy adhesives, before and after the aging treatments, Compos. Struct. 171 (2017) 145–157 https://doi.org/, doi:10.1016/j.compstruct.2017.03.020.
[14] J Lopes, D Stefaniak, L Reis, PP. Camanho, Single lap shear stress in hybrid CFRP/Steel composites, Procedia Struct Integr 1 (2016) 58–65 https://doi.org/, doi:10.1016/j.prostr.2016.02.009.
[15] HTN Kuan, WJ Cantwell, M a. Hazizan, C. Santulli, The fracture properties of environmental-friendly fiber metal laminates, J. Reinf. Plast. Compos. 30 (2011) 499–508 https://doi.org/, doi:10.1177/0731684411398536.
[16] P Wambua, B Vangrimde, S Lomov, I. Verpoest, The response of natural fibre composites to ballistic impact by fragment simulating projectiles, Compos. Struct. 77 (2007) 232–240 https://doi.org/, doi:10.1016/j.compstruct.2005.07.006.
[17] C Santulli, HT Kuan, F Sarasini, I De Rosa, W. Cantwell, Damage characterisation on PP-hemp/aluminium fibre–metal laminates using acoustic emission, J. Compos. Mater. 47 (2013) 2265–2274 https://doi.org/, doi:10.1177/0021998312457098.
[18] RDSG Campilho, DC Moura, DJS Gonçalves, JFMG Da Silva, MD Banea, LFM Da Silva, Fracture toughness determination of adhesive and co-cured joints in natural fibre composites, Compos. Part B Eng. 50 (2013) 120–126 https://doi.org/, doi:10.1016/j.compositesb.2013.01.025.
[19] S Budhe, MD Banea, S de Barros, LFM. da Silva, An updated review of adhesively bonded joints in composite materials, Int. J. Adhes. Adhes. 72 (2017) 30–42 https://doi.org/, doi:10.1016/j.ijadhadh.2016.10.010.
[20] LFM da Silva, RJC Carbas, GW Critchlow, MAV Figueiredo, K. Brown, Effect

of material, geometry, surface treatment and environment on the shear strength of single lap joints, Int. J. Adhes. Adhes. 29 (2009) 621–632 https://doi.org/, doi:10.1016/j.ijadhadh.2009.02.012.

[21] EM Moya-Sanz, I Ivañez, Garcia-Castillo SK, Effect of the geometry in the strength of single-lap adhesive joints of composite laminates under uniaxial tensile load, Int. J. Adhes. Adhes. 72 (2017) 23–29 https://doi.org/, doi:10.1016/j.ijadhadh.2016.10.009.

[22] PNB Reis, JAM Ferreira, F. Antunes, Effect of adherends rigidity on the shear strength of single lap adhesive joints, Int. J. Adhes. Adhes. 31 (2011) 193–201 https://doi.org/, doi:10.1016/j.ijadhadh.2010.12.003.

[23] LCS. Nunes, Shear modulus estimation of the polymer polydimethylsiloxane (PDMS) using digital image correlation, Mater. Des. 31 (2010) 583–588 https://doi.org/, doi:10.1016/j.matdes.2009.07.012.

[24] G Sun, X Liu, G Zheng, Z Gong, Q. Li, On fracture characteristics of adhesive joints with dissimilar materials – An experimental study using digital image correlation (DIC) technique, Compos. Struct. 201 (2018) 1056–1075 https://doi.org/, doi:10.1016/j.compstruct.2018.06.018.

[25] DC Moreira, LC. Nunes, Experimental analysis of bonded single lap joint with flexible adhesive, Appl. Adhes. Sci. 2 (2014) 1–8 https://doi.org/, doi:10.1186/2196-4351-2-1.

[26] E Sarlin, M Apostol, M Lindroos, VT Kuokkala, J Vuorinen, T Lepistö, et al., Impact properties of novel corrosion resistant hybrid structures, Compos. Struct. 108 (2014) 886–893 https://doi.org/, doi:10.1016/j.compstruct.2013.10.023.

[27] T Pärnänen, M Kanerva, E Sarlin, O. Saarela, Debonding and impact damage in stainless steel fibre metal laminates prior to metal fracture, Compos. Struct. 119 (2015) 777–786 https://doi.org/, doi:10.1016/j.compstruct.2014.09.056.